Elastic and inelastic proton scattering of ^{21}Na in inverse kinematics

David Jenkins, Adam Tuff

THE UNIVERSITY of York

DREB 2012

Outline

The X-Ray Burster Scenario, HCNO Cycles & Breakout: High energy scenarios: Red giant/Neutron star systems, mass accretion and **T**hermo-**N**uclear **R**unaway. **Hot C**arbon-**N**itrogen-**O**xygen cycle, competing breakout paths, the **RP**-process.

^{18}Ne(α,p) / ^{21}Na(p,p') reactions: Astrophysical importance, implications, past experimental difficulties / unknowns. Use of **inverse kinematics & radioactive beams** to probe states in ^{22}Mg.

Development of data sort code and analysis: Methodology – TIGRESS / BAMBINO. Gamma-ray gating, resonance spectra – particle angular distributions.

Simulation of experimental data, simulation of angular distributions – comparison to data. Potential assignments to states.

Reaction rates

X-Ray burster scenario

- The **^{18}Ne(α,p) ^{21}Na** reaction - breakout from the Hot-CNO cycle in X-Ray Bursters (**XRBs**). At high T bypasses **^{15}O(α,γ)**.
- Nucleosynthesis of **proton rich isotopes** from the rp-process. Affects energy generation in these environments.
- **Dominant reactions, cross-sections, resonances and properties unknown**.

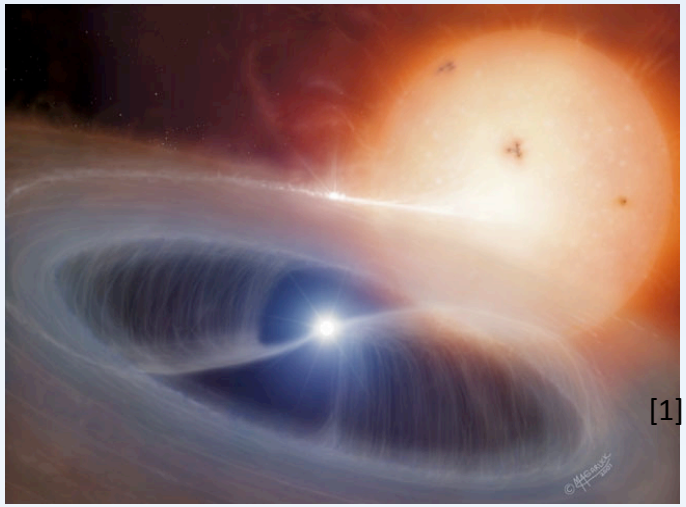

[1]

- Binary star system - Red giant and a neutron star (figure). Red giant fills **Roche lobe** - matter falls into the neutron star accretion disk before surface.

- Matter **electron degenerate** – T increases as H and He deposit on neutron star - leads to thermal instabilities and runaway reactions at above $T_9 > 0.5$ (5×10^8K)

"Breakout" from H-CNO cycle into rp-process at **$T_9 \geq 1$** – heavy element synthesis.

Hot-CNO cycle and breakout

Main generation in Novae dominated by **Hot-CNO cycle** at $T_9 < 0.4$ [3]. Nucleosynthesis dictated by "waiting points".

Competition between (p,γ), (α,p), (α,γ) and ($\beta^+\nu$). **Breakout occurs through $^{15}O(\alpha,\gamma)^{19}Ne$** path ($\tau_{1/2}$ = 122.2s, $T_9 > 0.4$)

For $T_9 > 0.8$, energetic α's: reaction rates increase. **$^{18}Ne(\alpha,p)$ bypasses** $^{15}O(\alpha,\gamma)^{19}Ne$ alters abundance.

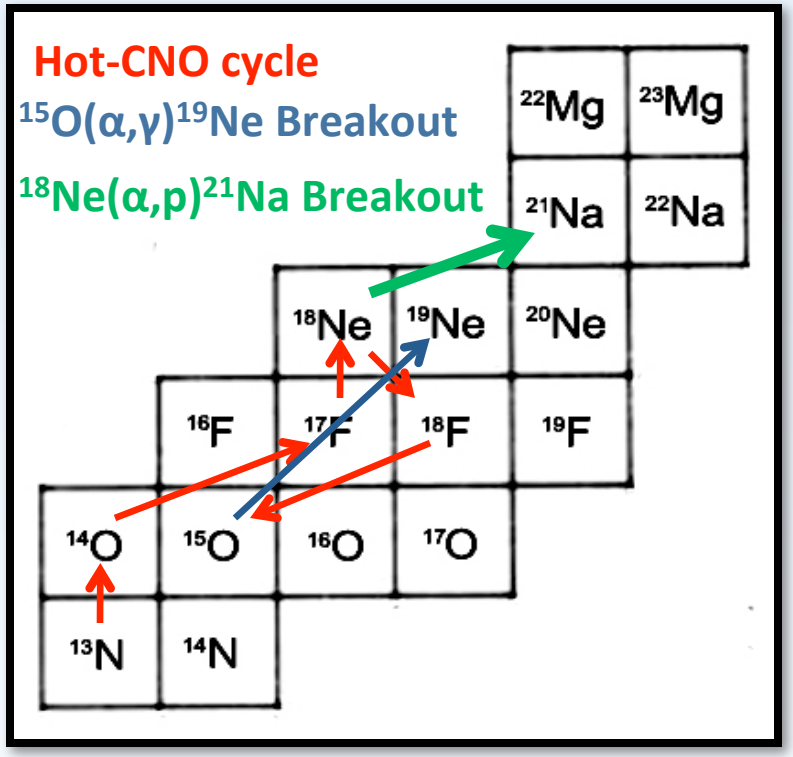

Energy generation proceeds through **rp-process**; proton captures / β^+-decays to heavier "proton rich" isotopes.

Inconsistency in existing literature

Difficult to produce high intensity ^{18}Ne beams ($\tau_{1/2}$ = 1.67s). Higher energy beams only thoroughly probe energy regions above 10.5MeV [Görres et al., 1995] - $T_9 \approx 1.5$.

Radioactive targets not suitable / practical.

Previous work by Bradfield-Smith et al., Sinha et al., Groombridge et al., using direct and time-reversed reactions are in conflict

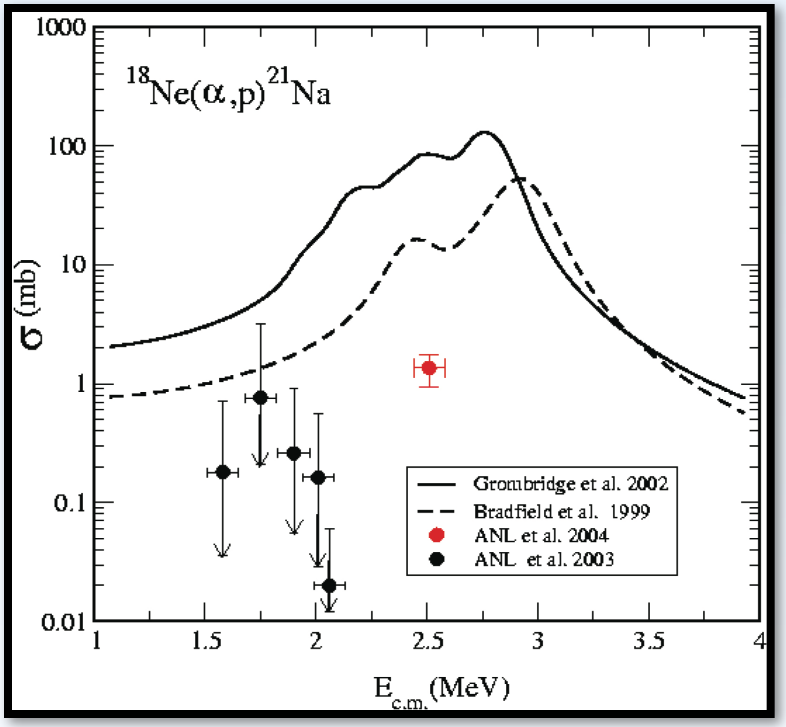

Energy levels in the "Astrophysically important" region above 8.14MeV (the α-particle threshold) in ^{22}Mg have been identified; key resonances, widths, spins etc... have not.

Level hunting

Further work published 2009 by Matic *et. al.* using a $^{24}Mg(p,t)^{22}Mg$ transfer reaction using Grand Raiden, RCNP, Osaka.

5 new states above the alpha-particle threshold

No spin/parities measured but inferred from mirror symmetry (questionable how useful that is in this region)

Rates calculated are shown to be higher than other reaction rates calculated previously even within temperature region examined.

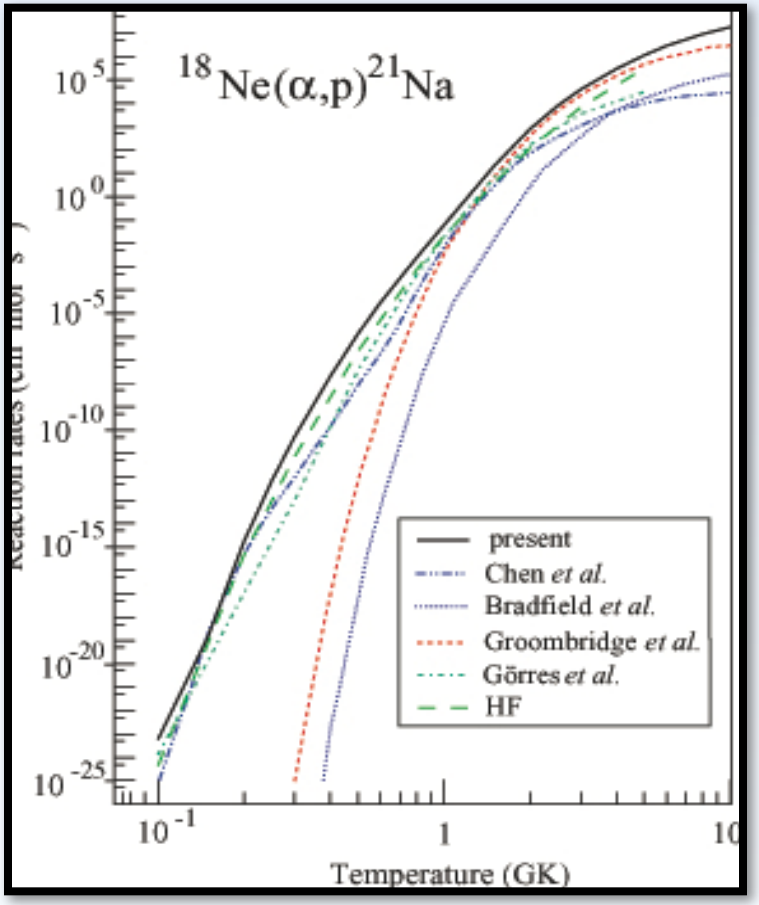

Indirect reaction

Proton scattering on ^{21}Na forms a ^{21}Na+p system. (^{21}Na proton threshold = 5.502MeV). The experimental spectrum is equivalent to level scheme in normal kinematics.

Level scheme by Chen *et al.* shows several states identified in the region of interest above the alpha-particle threshold.

Fire ^{21}Na beam at polyethylene target $(CH_2)_n$. Resonances in energy range through target (range from dE/dx): cross-section of detected protons increases: target does the "stepping".

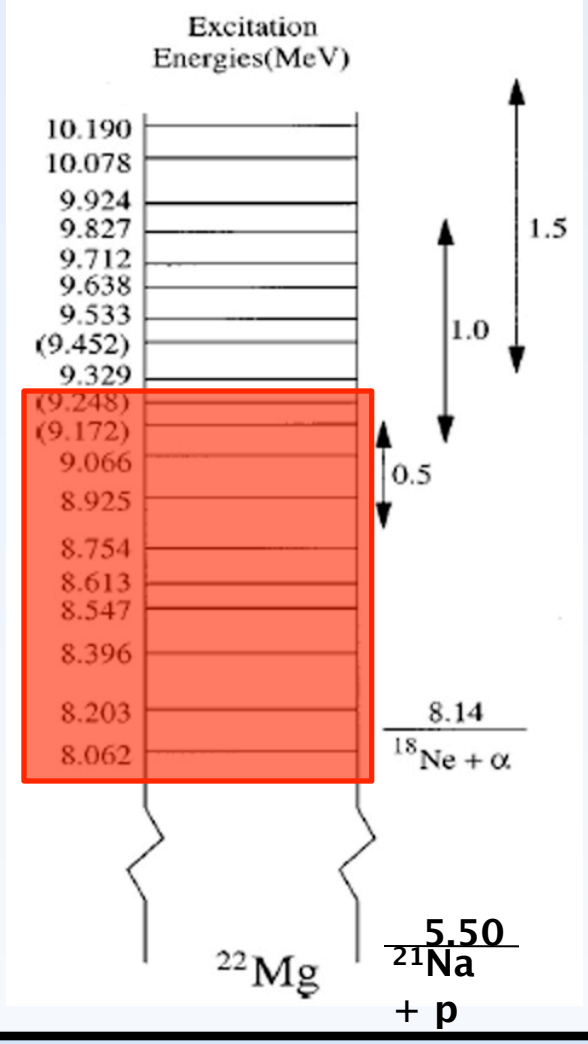

Experimental setup

^{21}Na interacts with target – scatters proton elastically/inelastically.
Proton detected in segmented ΔE-E detector: get trajectory & energy.
^{21}Na* γ-decays: TIGRESS detects 332keV γ's.

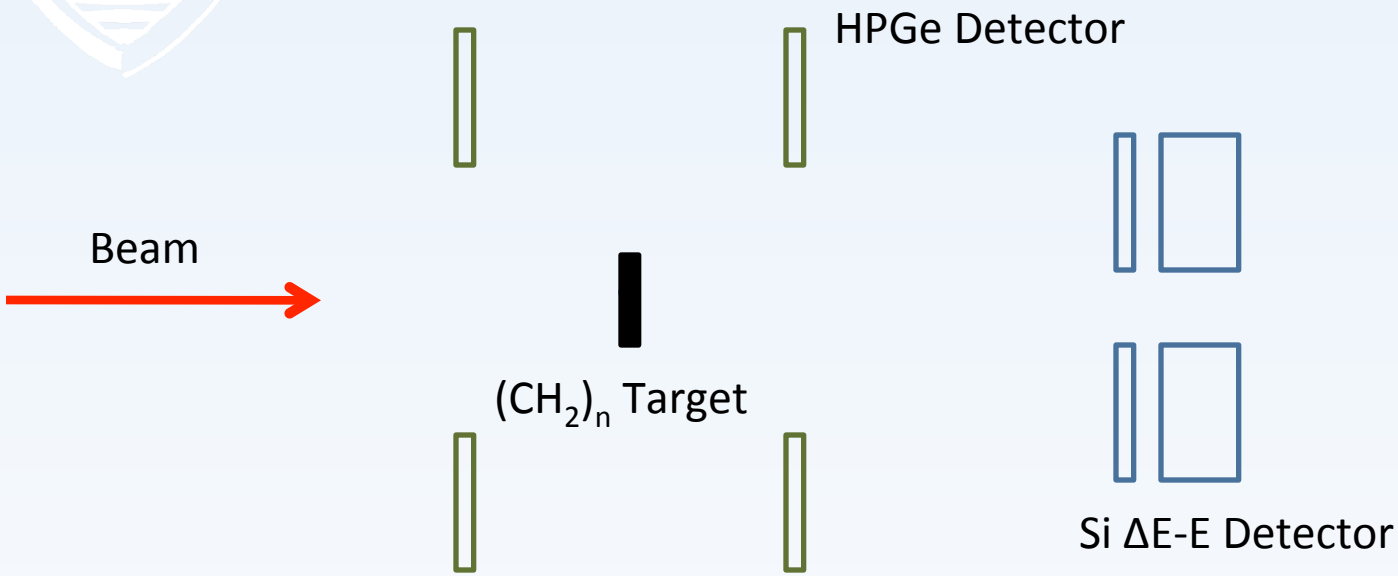

Experimental setup II

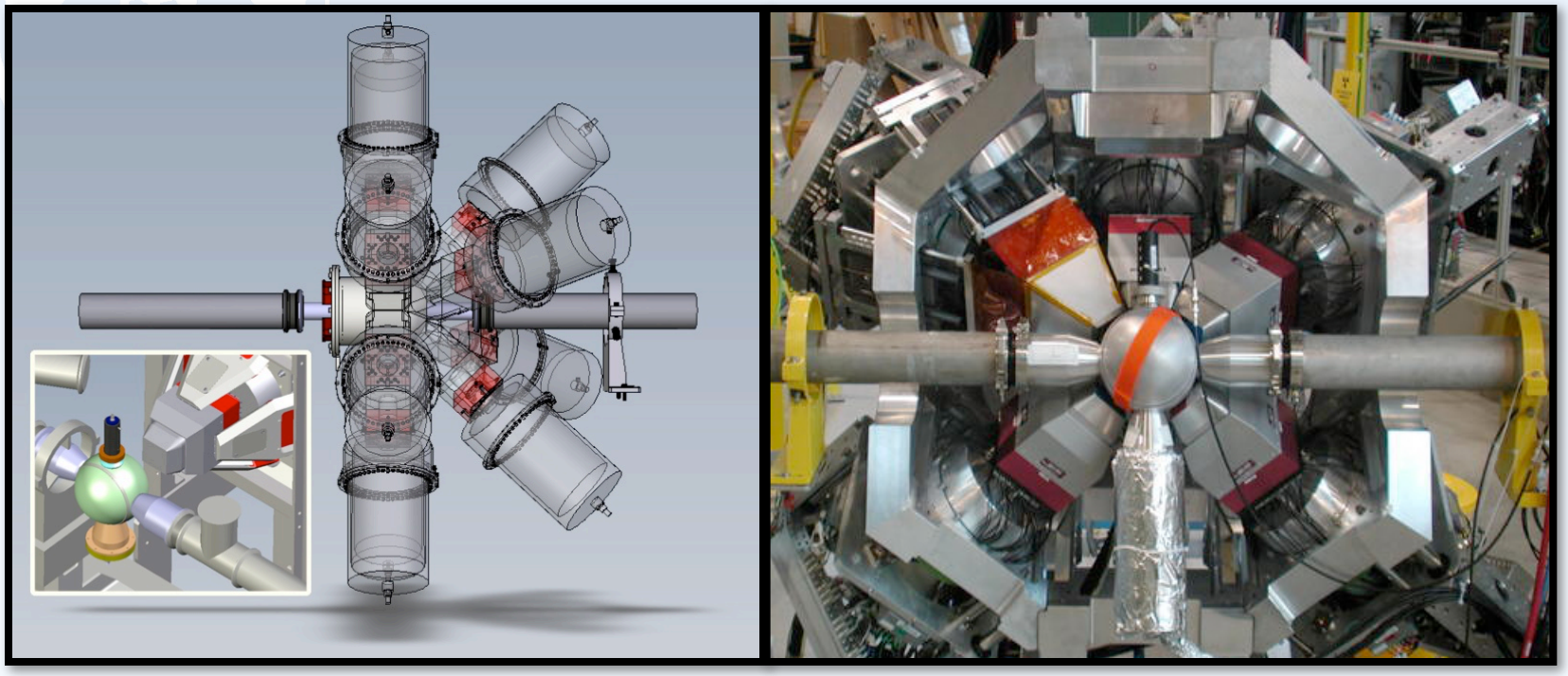

CAD design by F Cifarelli of TRIUMF, Vancouver. Image 2 courtesy of Greg Hackman and Douglas Cline.

Experimental setup III

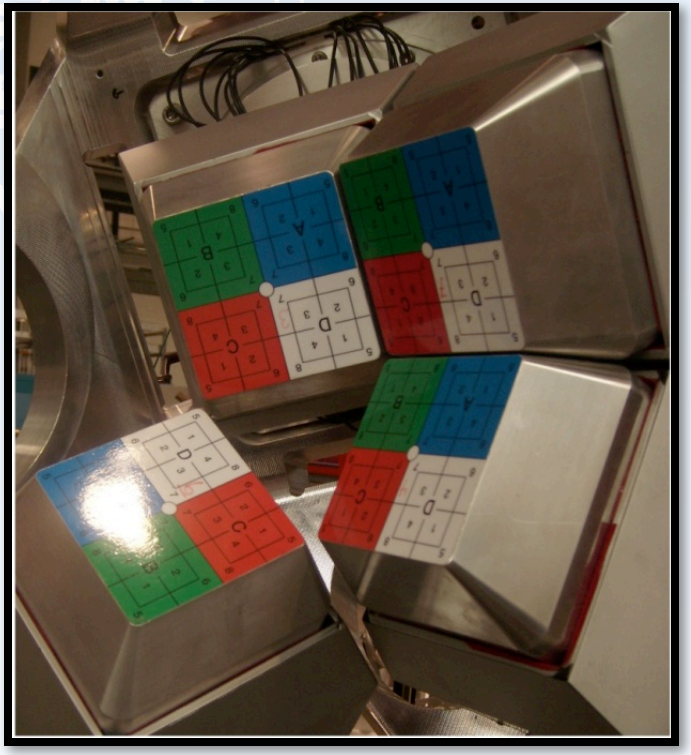

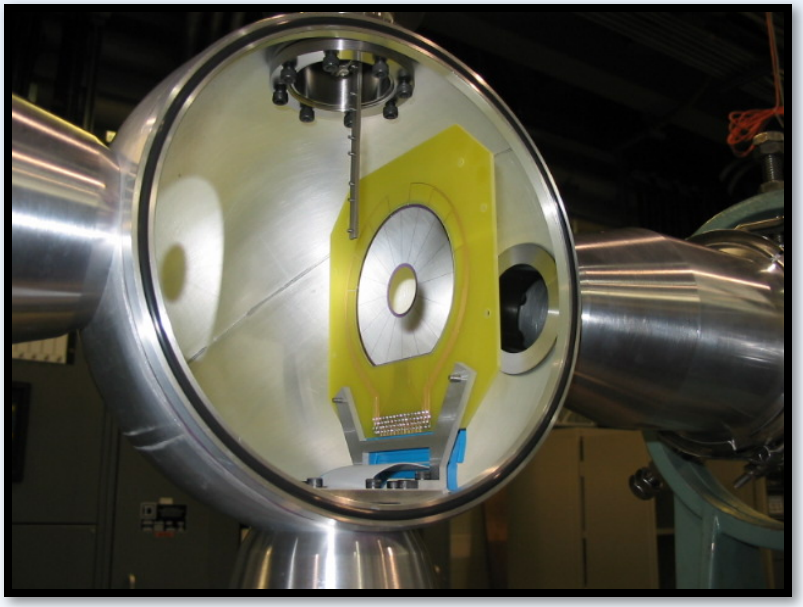

TIGRESS cluster and BAMBINO target ladder photos by Adam Tuff (UoY) and Greg Hackman (TRIUMF).

ΔE-E spectra

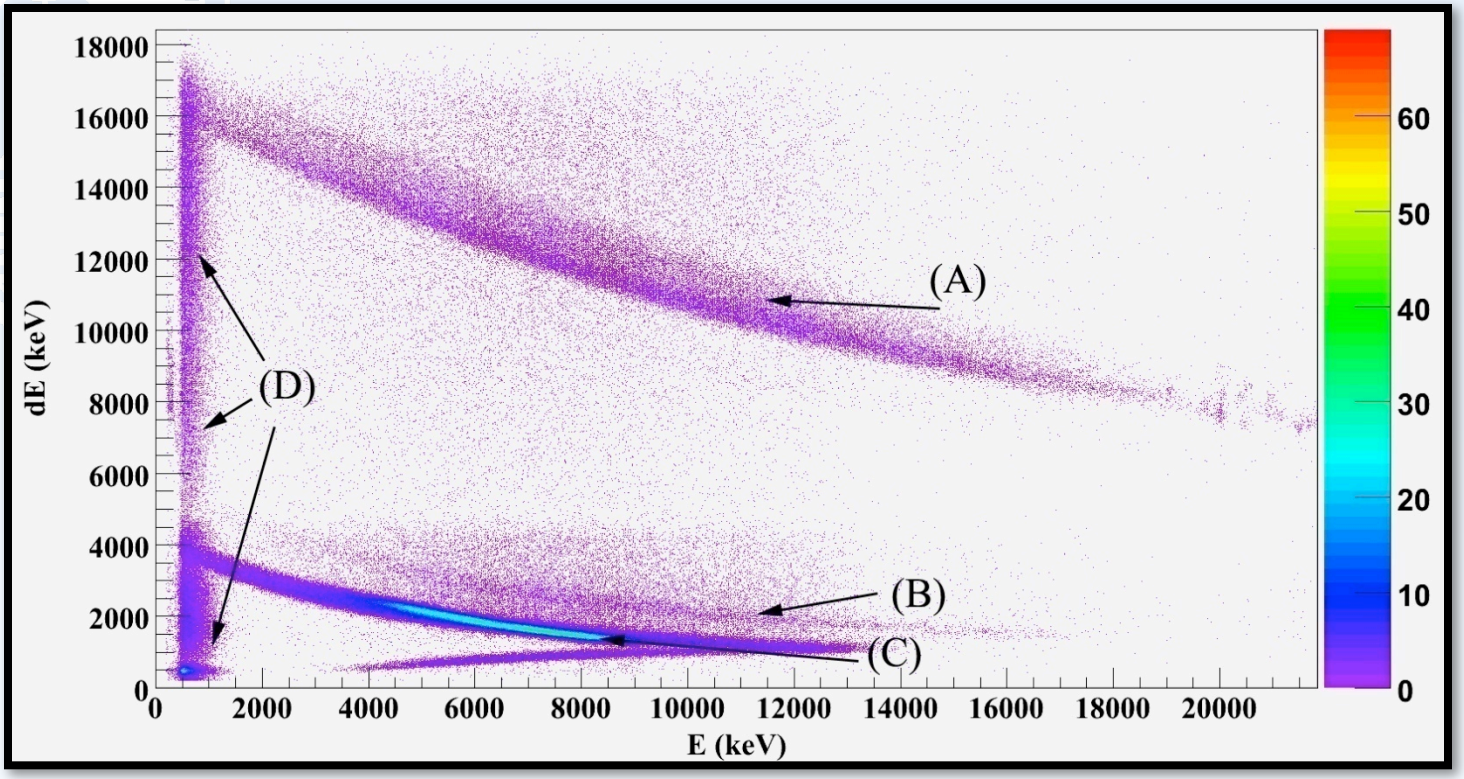

A) ^{4}He **B)** ^{2}H **C)** Elastic/Inelastic proton

Selecting the inelastic branch

Gamma-ray spectra after gating on BGOs, Timestamps, and coincidences.

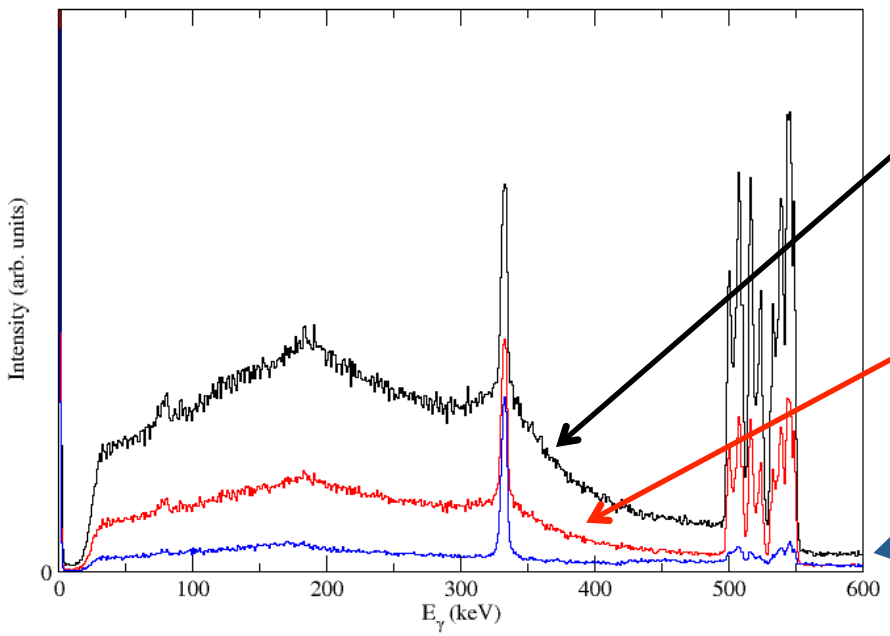

Raw spectra after Doppler corrections.

BGO events reject any scattered γ-ray events. Time stamp on particle and γ-ray events included.

Addback now included for single and multiple events. Si ring & sector gates on proton events now accounted allows further b/g reduction.

Separating fusion background

Small energy corrections for Si detector dead layer & Al doping (Simulated in SRIM & TRIM) – compared to energy variation as function of angle in calibration data. Dead layer found to be within manufacture tolerances.

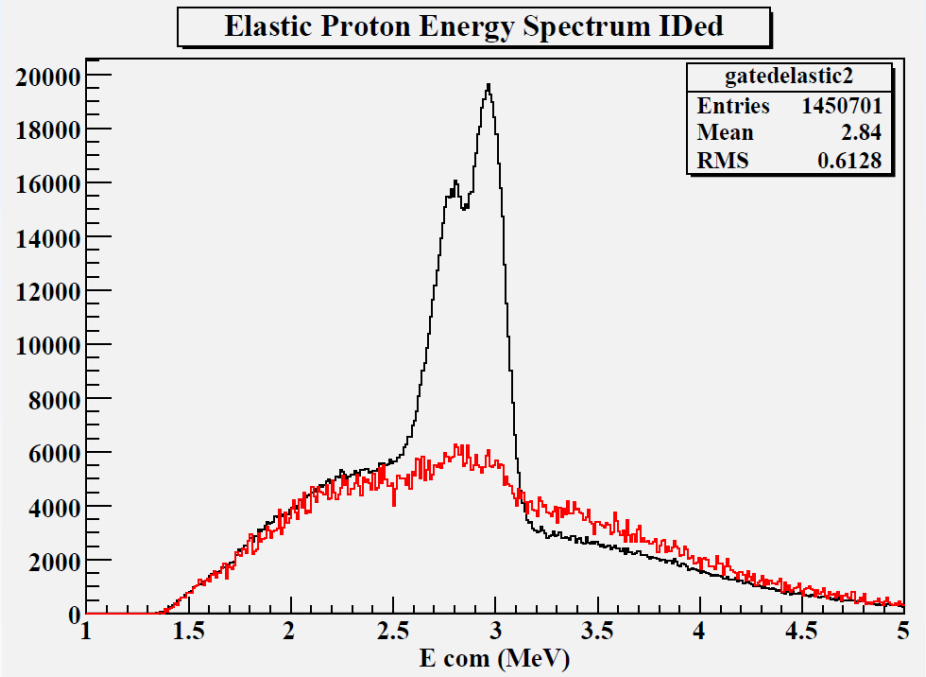

Proton spectra gated on ΔE-E.

Spectrum includes a proton background (due to fusion evaporation with carbon in target).

Similar to inelastic events, gate on γ–ray events associated with fusion events, scaled produces a background spectra which can be removed from the spectra.

Sample data

Elastic (a) & inelastic (b) proton spectra (c.m. energy) – run at 2.85MeV/u.

No resonance in spectra.

Software gate allows isolation of coincidence events with 332keV gamma-rays.

Black: Raw spectrum gated on proton events.
Blue: Inelastic proton events gated on gamma-ray events.
Red: Inelastic events corrected into c.m. Frame.

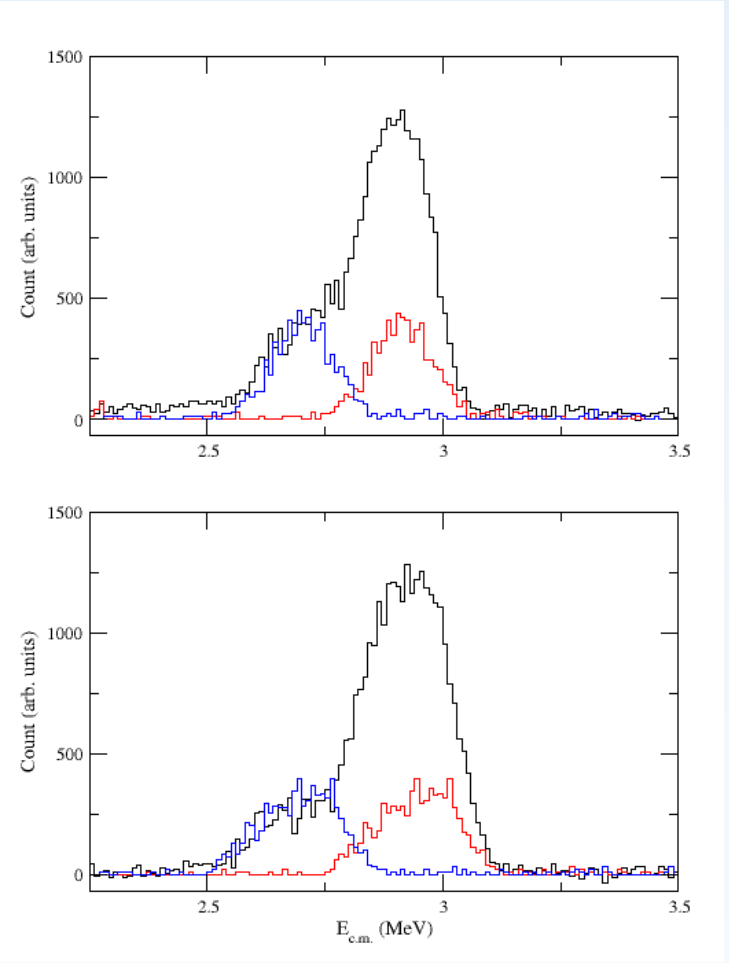

Resonance data

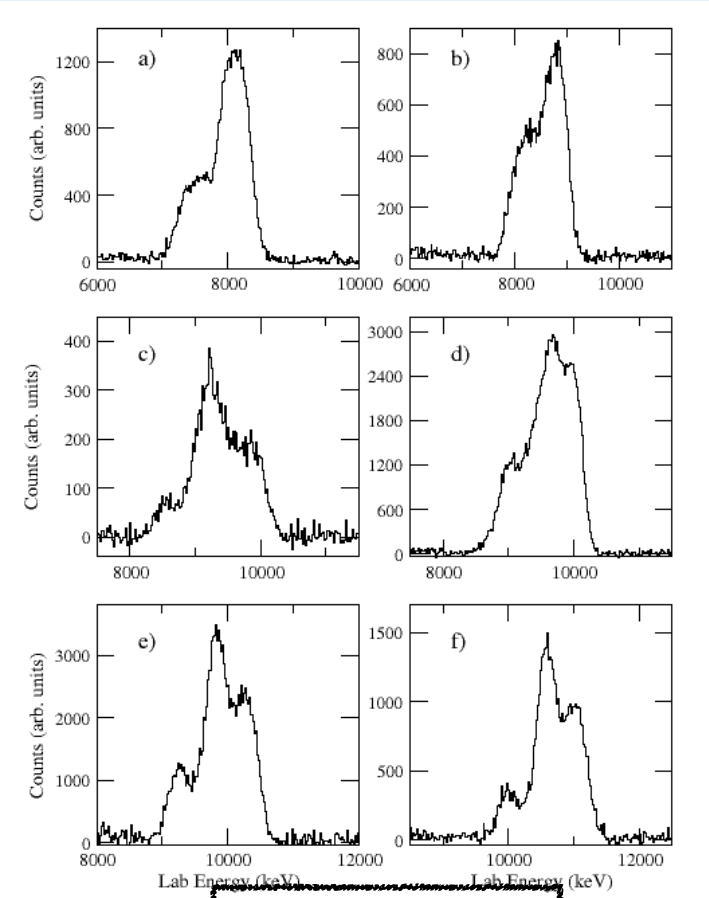

All energies studied

One resonance at different angles

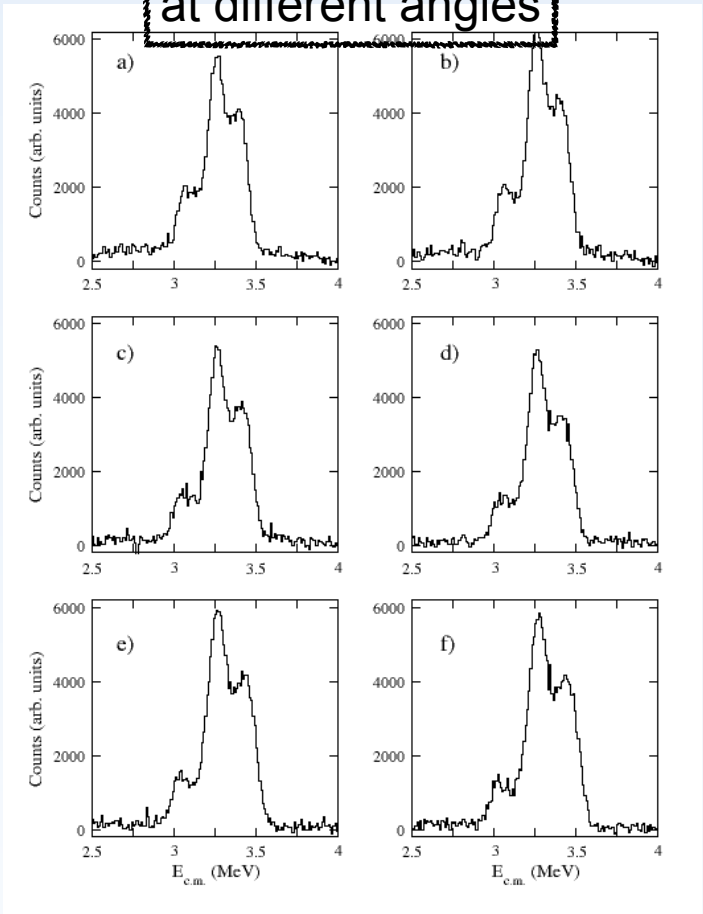

Angular distributions

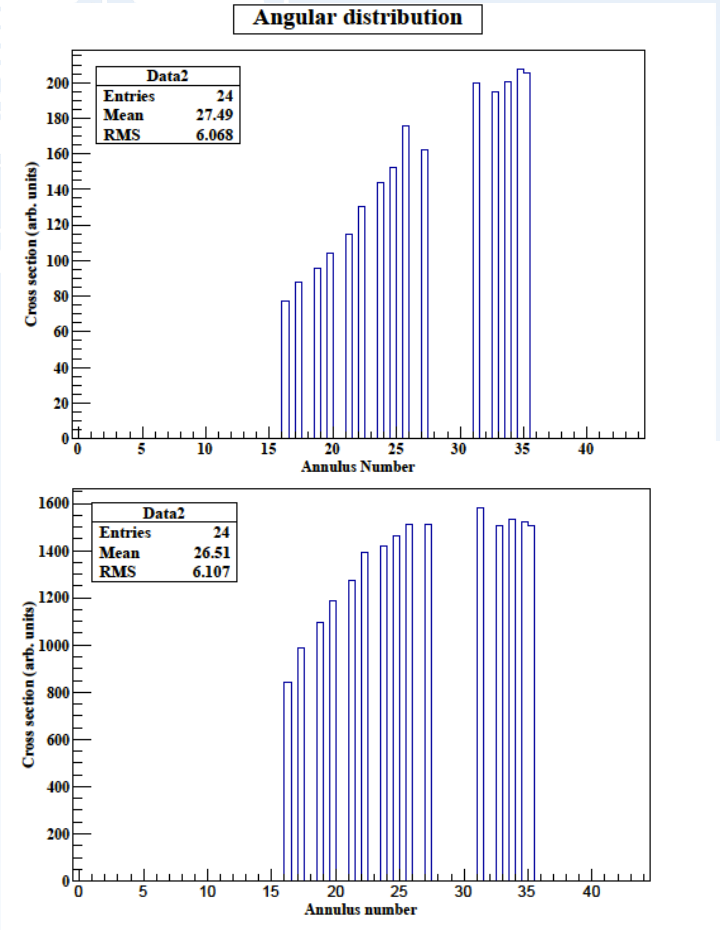

Examples of measured angular distributions as a function of ring number (increasing lab angle / decreasing cm angle) over resonances.

Both resonances (top resonance @ 3.054 MeV c.m., bottom @ 3.191 MeV c.m.) display very different distributions.

Indicates these states are likely to be of differing spin-parities.

Resonance simulation

$$
\begin{aligned}
d\sigma_{\alpha\alpha} \;=\;& z^2 \mathrm{cosec}^4(1/2\theta)\; d\Omega \\
&+ \frac{\lambda_\alpha{}^2}{(2I+1)(2i+1)} \sum_{L=0}^{L_{\max}} R_L(\alpha,\alpha)\; P_L(\cos\theta)\; d\Omega \\
&- 2\lambda_\alpha z \sum_{l=0}^{\infty} (2l+1)\; \sin\phi_l\; \cos\left[2\eta\; \ln\left[\sin(1/2\theta)\right] + 2\psi_l + \phi_l\right] \\
&\times \mathrm{cosec}^2(1/2\theta)\; P_l(\cos\theta)\; d\Omega \\
&+ \lambda_\alpha^2 \sum_{L=0}^{\infty} \sum_{l=0}^{\infty} \sum_{l'=l-L}^{l+L} (2l+1)(2l'+1) \left[(l_1 l_2 00 | l_1 l_2 L0)\right]^2 \sin\phi_l\; \sin\phi_{l'} \\
&\times \cos\left[(2\psi_l + \phi_l) - (2\psi_{l'} + \phi_{l'})\right] P_L(\cos\theta)\; d\Omega \\
&+ \frac{\lambda_\alpha (2J_0+1)}{(2I+1)(2i+1)} \sum_{l'=l_{\min}}^{J_0+I+i} \frac{\Gamma_{\alpha l}}{\left[(E-E_0)^2 + (1/2\Gamma)^2\right]^{1/2}} \mathrm{cosec}^2(1/2\theta) \\
&\times \sin\left[2\eta\; \ln\,\sin(1/2\theta) + 2\psi_l + \phi_l + \beta\right]\; P_l(\cos\theta)\; d\Omega \\
&- \frac{\lambda_\alpha{}^2 (2J_0+1)}{(2I+1)(2i+1)} \sum_{L=0}^{\infty} \sum_{l'=l_{\min}}^{J_0+I+i} \sum_{l'=|l-L|}^{l+L} (2l'+1) \left[(ll'00 | l'L0)\right]^2 \sin\phi_{l'} \\
&\times \frac{\Gamma_{\alpha l}}{\left[(E-E_0)^2 + (1/2\Gamma)^2\right]^{1/2}} \sin(\beta + 2\psi_l + 2\phi_l - 2\psi_{l'} - 2\phi_{l'})\; P_L \cos\theta\; d\Omega
\end{aligned}
$$

Blatt and Biedenharn, Rev. Mod. Phys. 24, 258 (1952)

Resonance components

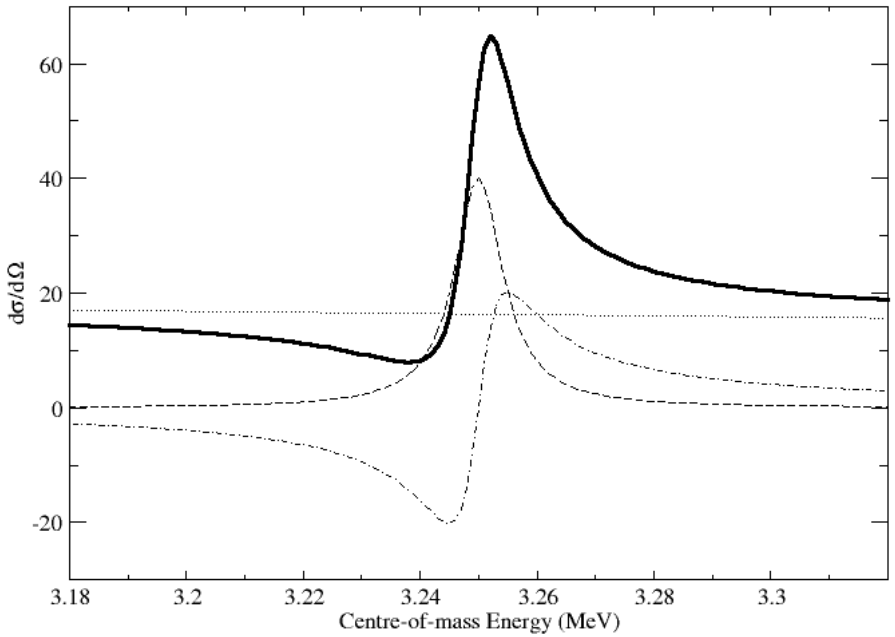

Resonance simulation comprised of six components:

- Coulomb / Rutherford
- Resonance (BW)
- Hard sphere corrections (x2)
- Interference terms (x2)

Example resonance

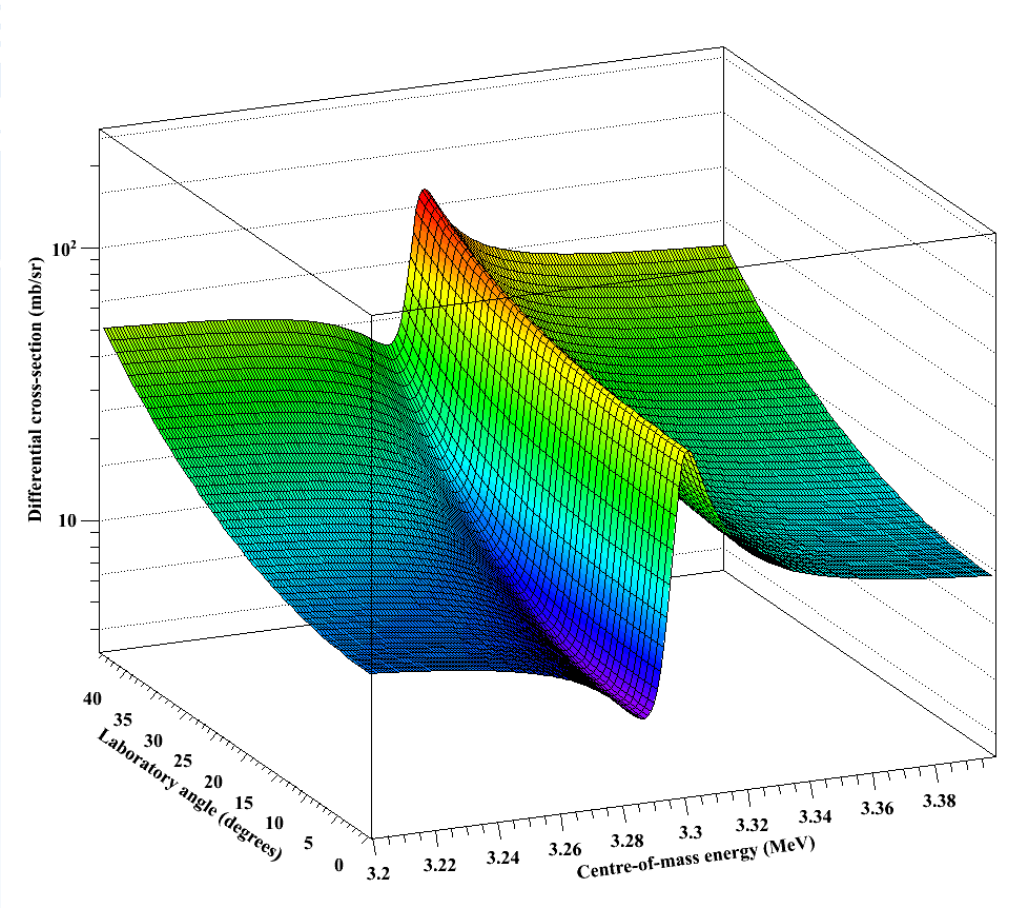

Angular distributions for different J^p

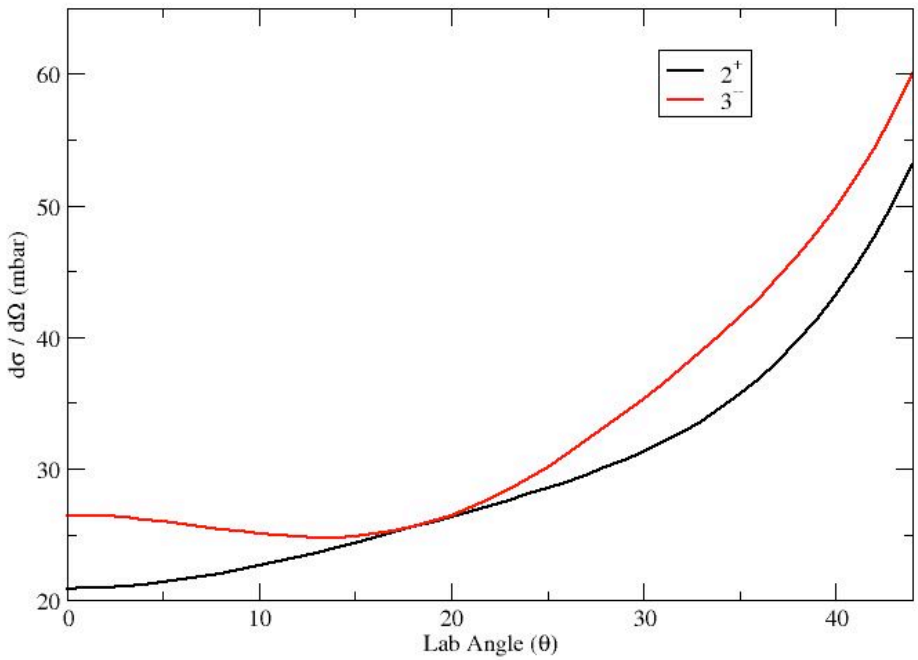

Simulated distribution across resonances (cross-sections are completely arbitrary here).

Positive and negative parity states / spins display differing distributions.

Should be able to determine resonance parity at least from distributions (work ongoing).

Reaction rates

Determination of resonance strengths – comprised of two components – statistical spin factor and width ratio (along with energy-dependence):

$$\omega\gamma = \frac{2J+1}{(2J_1+1)(2J_2+1)}(1+\delta_{12})\frac{\Gamma_a\Gamma_b}{\Gamma}.$$

Spin assignment important two fold here:

1) Statistical spin factor weighting.
2) Alpha particle widths – as these are much smaller than the proton widths for the direct reaction (^{18}**Ne(α,p)** ^{21}**Na**) they dominate this component.

    - this goes as penetrability (very sensitive) – therefore calculation of this **very** dependent on orbital angular momentum.

Alpha cluster states?

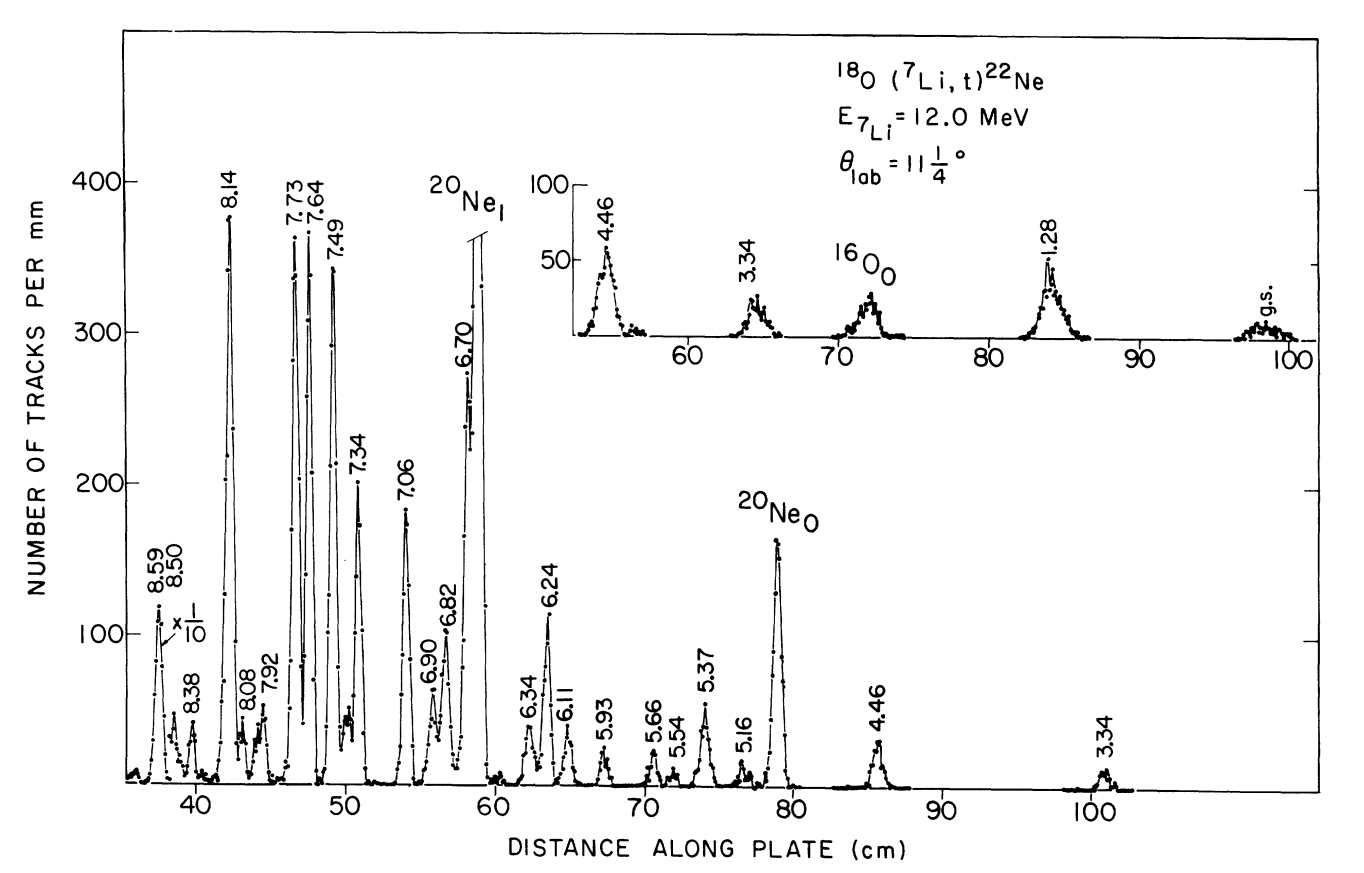

Scholz et al., Phys. Rev. C 6, 893 (1972)

Summary and near-future plans

Four resonances observed
Inelastic branch can be separated but appears to be small (much smaller than earlier (a,p) studies - why?)

Matching resonance angular distributions to obtain spin-parity assignments.
Angular distributions for inelastic channels (not sure how to treat)
Determine key states.
Compute revised reaction rates for the astrophysical scenario.

Elastic and inelastic proton scattering of ^{21}Na in inverse kinematics

D.G. Jenkins[1], A.G. Tuff [1], A.P. Robinson[10], C.Aa. Diget[1], O.J. Roberts[1] G. Hackman[2] , R.A.E. Austin[3], T. Davinson[4], P.J. Woods[4], G. Lotay[4], C. Pearson[2], A. Shotter[2], M. Schumaker[5], A.B. Garnsworthy[2], C. Svensson[5], C.Y. Wu[6], S. Williams[2], N. Orce[2], D.S. Cross[2], R. Kshetri[2], N. Galinski[7], T.E. Drake[8], R. Kanungo[3], S.J. Rigby[9], M. Jones[9], H. al Falou[3], C. Sumithrarachi[5], S. Triambak[2], G. Ball[2]

[1] Department of Physics, the University of York, Heslington, York, YO10 5DD, UK
[2] TRIUMF, 4004 Wesbrook Mall, Vancouver, British Columbia, V6T 2A3, Canada
[3] Department of Astronomy and Physics, Saint Mary's University, Halifax Nova Scotia, B3H 3C3, Canada
[4] The School of Physics and Astronomy, The University of Edinburgh, James Clerk Maxwell Building, King's Buildings, Mayfield Road, Edinburgh, EH9 3JZ. UK
[5] Department of Physics, University of Guelph, Guelph, Ontario, N1G 2W1, Canada
[6] Lawrence Livermore National Laboratory , 7000 East Avenue, Livermore, CA 94550, California, USA
[7] Department of Physics & Astronomy, University of British Columbia , 6224 Agricultural Road, Vancouver, British Columbia, V6T 1Z1, Canada
[8] Department of Physics, University of Toronto, 60 St. George St., Toronto, M5S 1A7, Ontario, Canada
[9] Department of Physics, University of Liverpool, Liverpool, L69 7ZE, UK
[10] The School of Physics and Astronomy, The University of Manchester, Oxford Road, Manchester, M13 9PL, UK

A study of breakout from the Hot-CNO cycle in X-Ray bursters using inelastic proton scattering of 21Na in inverse kinematics

PRELIMINARY ANALYSIS

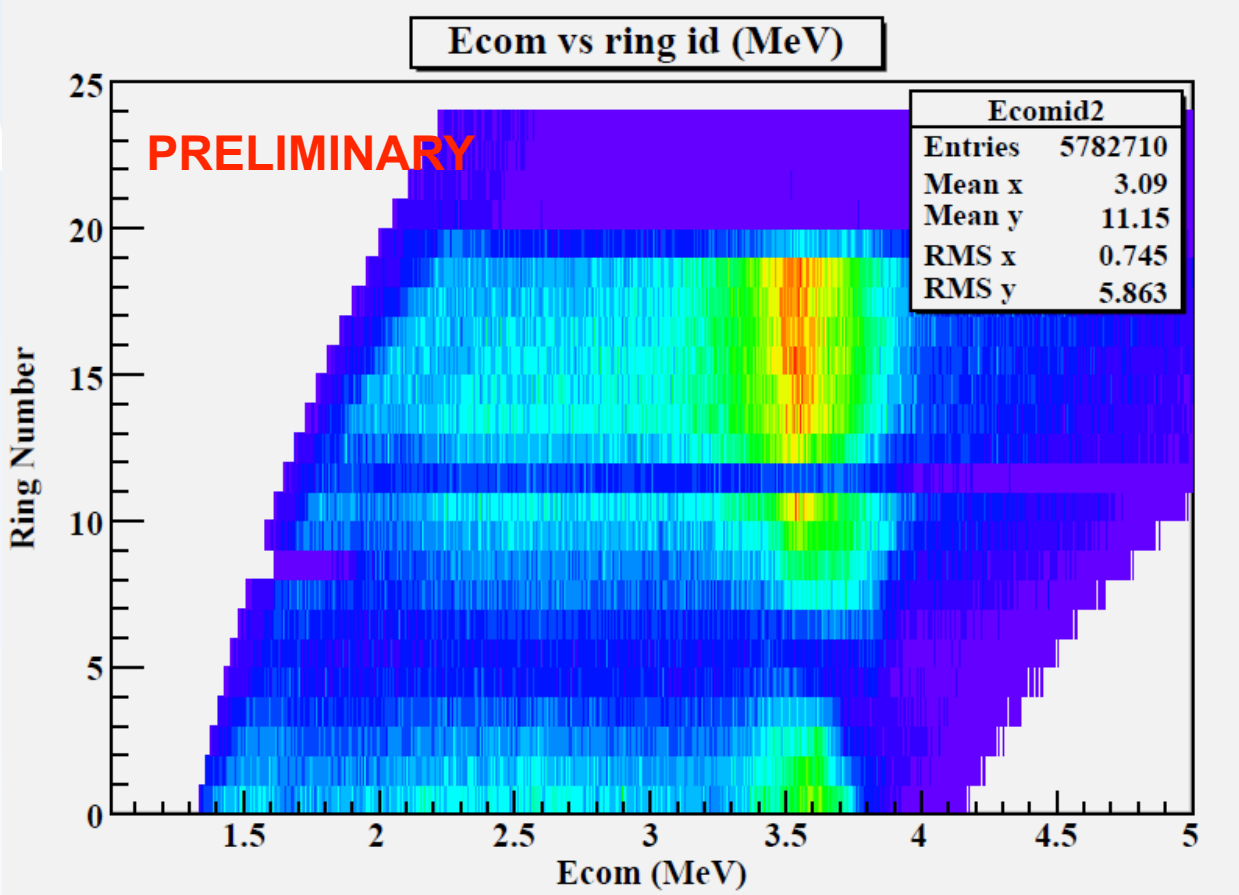

Run at 3.800MeV/u bombarding energy.

Resonance at 3.57MeV has differing angular distribution to the resonance at 3.32MeV (from 3.55MeV run).

May indicate different spin/parity.

A study of resonant states involved in breakout from the hot-CNO cycle using inelastic proton scattering of ^{21}Na in inverse kinematics

^{21}Na(p,γ)^{22}Mg REACTION

Above the CNO cycles lie the NeNa and MgAl cycles.

Breakout from these conditions into the rp-process depend on a) stellar temperatures and b) hydrogen densities in the environment.

Breakout from ^{19}Ne(p,γ)^{20}Na allows bypassing of NeNa cycle via ^{20}Na(p,γ)^{21}Mg – as it can compete with β-decay.

Main importance of study of rp-process is nucleosynthesis. In our case, rp-process is not important in seeding of the ISM – more important as a competing process to HCNO in energy generation in XRBs.

A study of resonant states involved in breakout from the hot-CNO cycle using inelastic proton scattering of ^{21}Na in inverse kinematics

PRELIMINARY ANALYSIS

Inelastic proton spectra (c.m. energy) – run at 3.1MeV/u.

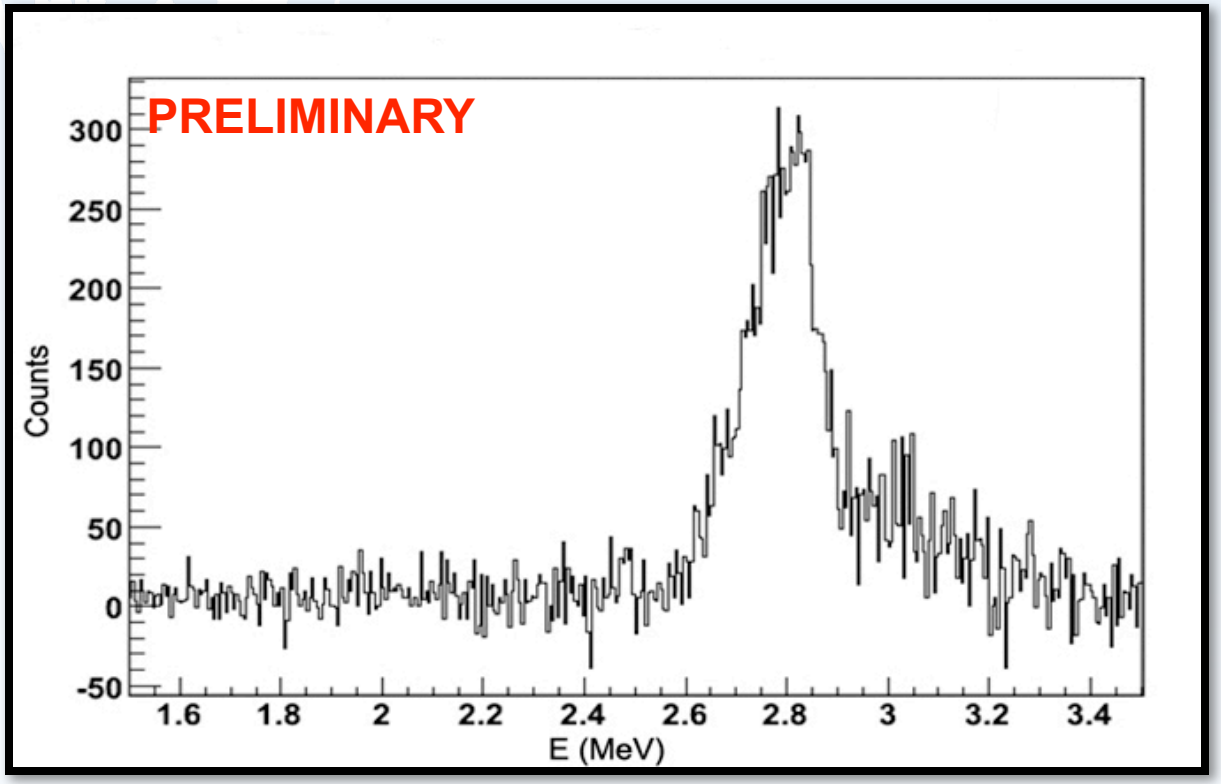

Peak here created by a large gate on the γ-ray spectra on the 332keV de-excitation.

Tighter gating will allow clean-up of this spectra.

Features will hopefully be more obvious with addition of more data (data taken from 30 minutes of a run).

A study of resonant states involved in breakout from the hot-CNO cycle using inelastic proton scattering of ^{21}Na in inverse kinematics

PRELIMINARY ANALYSIS

S2 and S3 Ring and Segment IDs for Proton events in BAMBINO (E-ΔE Si)

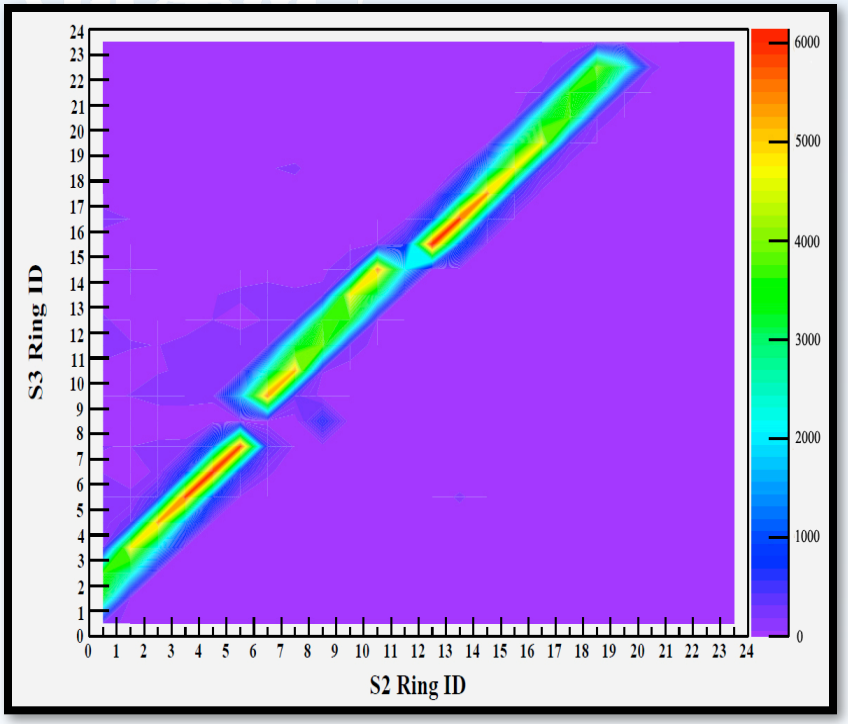

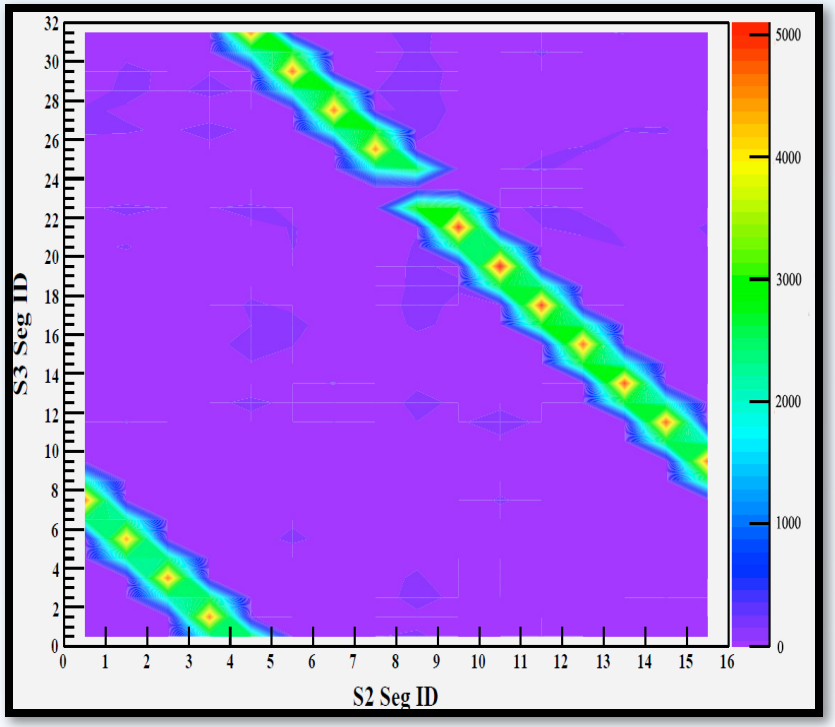

A study of resonant states involved in breakout from the hot-CNO cycle using inelastic proton scattering of ^{21}Na in inverse kinematics

PRELIMINARY ANALYSIS

Software developed for alpha particle calibrations of Si Detectors.

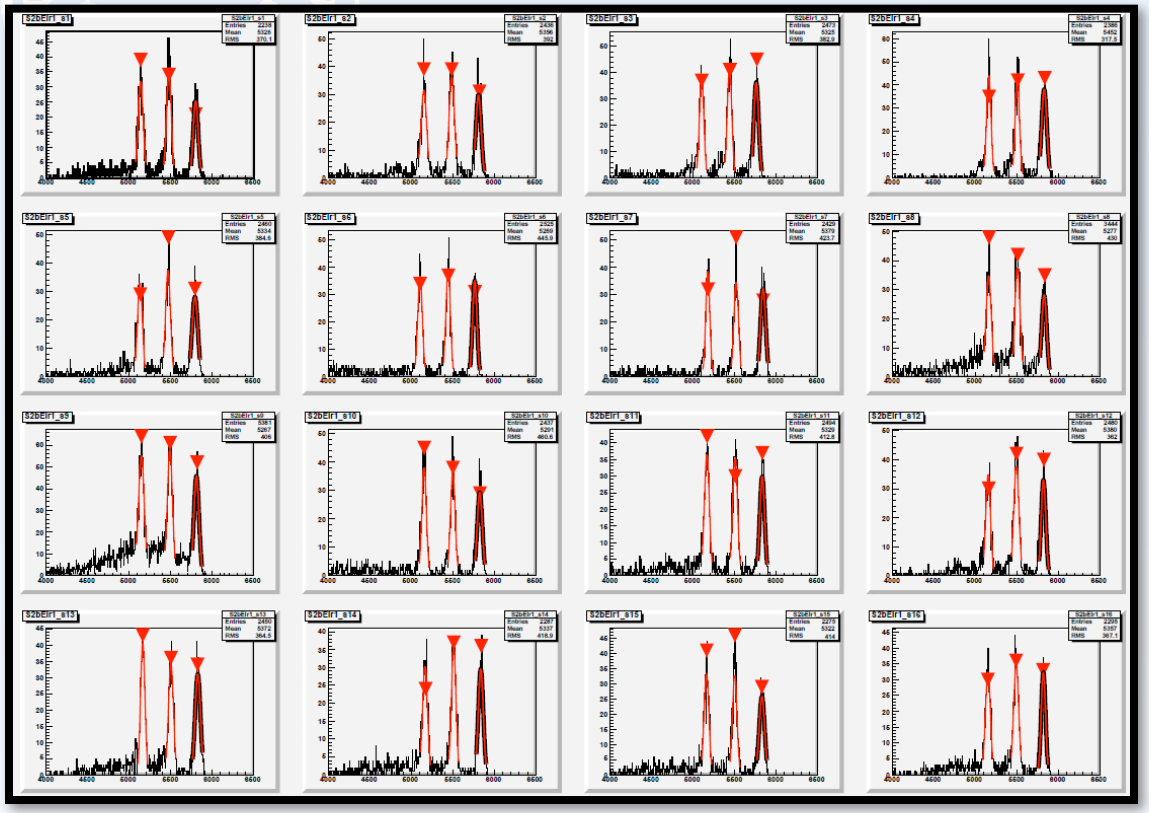

Identifies alpha particle energy peaks using a "peak-finder" routine – guide for region over which a Gaussian is fitted. calculates gain and offsets.

Outputs parameters in ascii format that can universally read by other codes for calibration of BAMBINO CD detectors.

Identifies low statistic and poor resolution channels.

A study of resonant states involved in breakout from the hot-CNO cycle using inelastic proton scattering of ^{21}Na in inverse kinematics

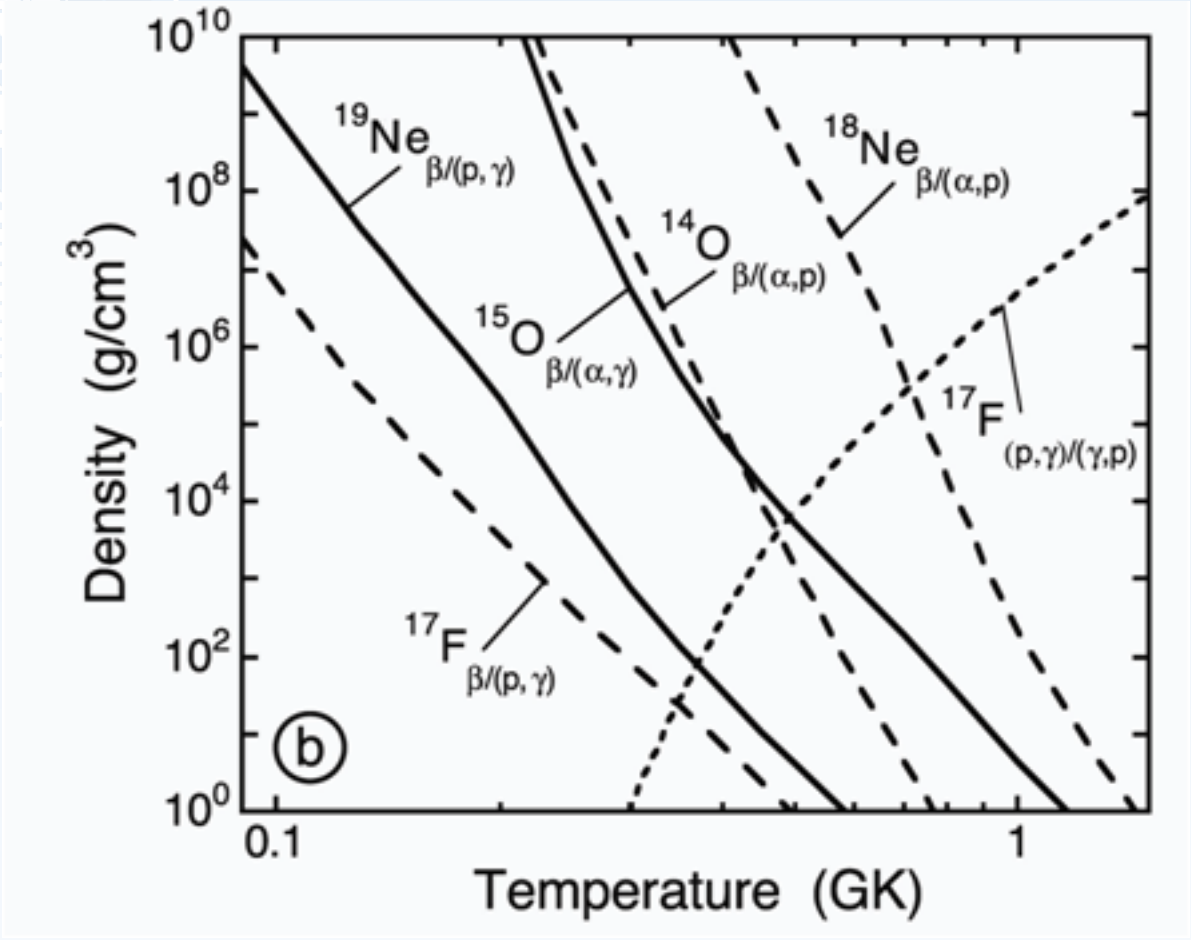

A study of breakout from the Hot-CNO cycle in X-Ray bursters using inelastic proton scattering of 21Na in inverse kinematics

EXPERIMENTAL MOTIVATION

The **^{18}Ne(α,p) ^{21}Na** reaction is considered to be a crucial process governing breakout conditions from the Hot-CNO cycle in X-Ray Bursters (**XRBs**) under certain stellar conditions – bypasses another breakout route via **^{15}O(α,γ) ^{19}Ne** at high temperatures.

Dictates further nucleosynthesis of **proton rich isotopes** from the rp-process in XRB sites, as well as energy generation in these environments.

Energy generation in explosive nuclear scenarios relatively unknown: rp-process and Hot-CNO cycle are both competing processes – **dominant reactions, cross-sections, resonances, and properties of resonant states** in these energy regions have not been identified.

Reaction Rates

Theoretical variation of reaction rate as a function temperature (normalised to $^{16}O(\alpha,\gamma)$) [9].

Predicts change in the $^{18}Ne(\alpha,p)$ cross-section by nearly four orders of magnitude between T_9 = 0.6 - 1.

Extremely sensitive to temperature variation.

Sensitivity to density of reactants.

Expected to exceed the $^{16}O(\alpha,\gamma)$ around T_9 = 0.8.

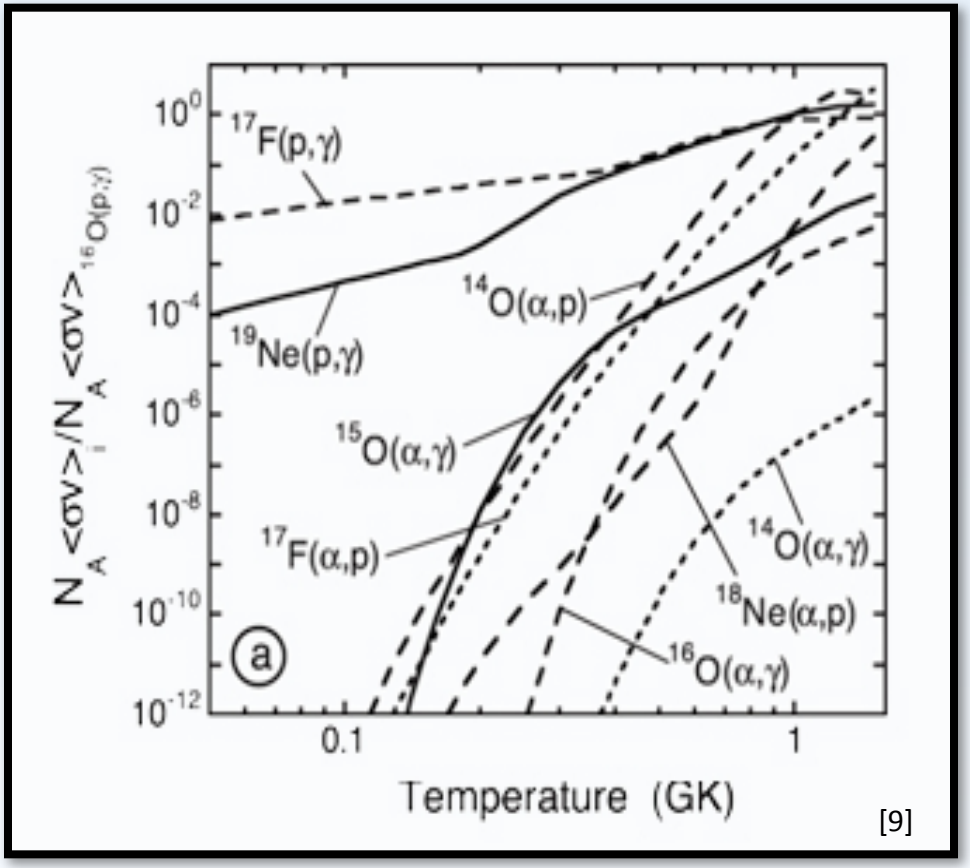

[9]

Resonance simulation

where

$$R_L(\alpha,\alpha) = \sum_{s=|I-i|}^{I+i} \sum_{s'=|I'-i'|}^{I'+i'} \frac{(-1)^{s'-s}\Gamma^2}{4(E-E_0)^2+(1/2\Gamma)^2} \sum_{l_1=|J_0-s|}^{J+s} \sum_{l_2=|J_0-s|}^{J+s}$$
$$\sum_{l_1'=|J_0-s'|}^{J+s'} \sum_{l_2'=|J_0-s'|}^{J+s'} Z(l_1 J_0 l_2 J_0, sL)\; Z(l_1' J_0 l_2' J_0, s' L)\; \cos\left[\xi_{l_1} - \xi_{l_2} + \xi_{l_1'} - \xi_{l_2'}\right]$$

where

$$Z(l_1 J_1 l_2 J_2, sL) = i^{L-l_1+l_2}(2l_1+1)^{1/2}(2l_2+1)^{1/2}(2J_1+1)^{1/2}(2J_2+1)^{1/2}$$
$$\times W(l_1 J_1 l_2 J_2, sL)(l_1 l_2 00|l_1 l_2 L0)$$

where

$$W(abcd;ef) = \Delta(abe)\Delta(acf)\Delta(bdf)\Delta(cde)\sum_z (-1)^z (a+b+c+d-1-z)!$$
$$\times[z!(e+f-a-d+z)!(e+f-b-c+z)!(a+b-e-z)!$$
$$\times(c+d-e-z)!(a+c-f-z)!(b+d-f-z)!]^{-1} \qquad \text{(D.5)}$$

and

$$|j_1 j_2 JM\rangle = \sum_{m_1 m_2} |j_1 j_2 m_1 m_2\rangle\langle j_1 j_2 JM\,|JM\rangle,$$